Noname manuscript No.
(will be inserted by the editor)

Modeling and Simulating the Dynamics of the "Death Star" Shotgun Target

Alexander A. Brown
Department of Mechanical Engineering
Lafayette College
Easton, PA, USA

July 18, 2016

Abstract Modern competitive shooting is a strenuous test of the human perceptual and motor systems. Like driving a race car or piloting a high performance aircraft, speed shooting matches require precise, rapid movements coordinated using a careful mixture of planning and reaction. In some disciplines of competitive shooting, this mixture is further complicated by complex moving targets. This paper develops a set of state space equations for a moving, reactive steel target used in professional 3-Gun competition. The equations for target motion are nonlinear, time-varying, and chaotic in certain regions of the state space. Once derived, the equations for target motion are validated against motion extracted from video. Then, the calibrated equations are implemented in real-time on a portable, laser-activated simulator. Applications of the simulation environment to marksmanship training and human motor control studies are also discussed.

1 Introduction

While it has received relatively light attention in the literature, competitive shooting is a sport rich in analogies to fundamental questions about human behavior and performance. Often, treatments of competitive shooting are approached from a cognitive science perspective [1–6] or are rooted physiology/biomechanics [7–11]. Many of these focus on bullseye-type shooting with either rifles or pistols, and a few, such as the work of Causer et al. in [1] or Share et al. in [8] focus on shotgun competition with flying clay targets. With the exception of studies concerning biathlon shooting, e.g. the work of Vickers and Williams in [5] or Baca & Kornfeind in [6], studies of shooting sports where speed and accuracy are both scored are scarce. In 3-Gun competition, competitors use rifle, pistol, and shotgun to complete courses of fire in the fastest time possible, and receive time penalties for misses. This paper will focus on the modeling, analysis, and simulation of a particular shotgun target introduced to professional 3-Gun shooting in 2015 by 3Gun Nation®, a regulatory body that produces a television show on the sport's professional circuit. The target's motion is particularly interesting because its motion is dynamic, and represents an opportunity to study human aiming in ways the human motor control community has not yet explored.

In general, hitting moving targets with a shotgun is an interesting blend of manipulandum control, perception, and prediction tasks. To be successful, a shooter must accurately point the shotgun, track a moving target, and predict its position at a future time in order to properly "lead" the target to ensure a hit. In [1], Causer et al. found links between "quiet eye" duration and skill at hitting moving targets with a shotgun. More generally speaking, the capture of moving targets has received a fair amount of attention, and generated a fair amount of disagreement in the human motor control field, with some researchers such as Hoffmann [12] finding evidence of "chasing" behavior, and others, such as Tresilian [13] advocating an ambush-type approach to target capture. Anecdotally, it seems that a blend of these approaches is employed when attempting to hit flying clay targets.

In constrast to clay target sports, however, which simulate hunting, professional 3-Gun shooting is scored based on elapsed time, and requires that competitors master a swinging, double-hinged target sporting five steel plates that the competitor knocks off of a star-

A.A. Brown
Lafayette College, 518 High Street, Easton PA 18042
E-mail: brownaa@lafayette.edu

shaped carrier. Figure 1 shows the "Death Star," as it has become colloquially known, in an action sequence. The target captures some of the peculiar behavior of the double pendulum, offering an element of unpredictability that makes shooting the target quickly extremely difficult. This unpredictability or "chaos" in the target dynamics arises not from random processes or uncertainty, but from the nonlinear equations' sensitivity to initial conditions [14]. Double pendulum systems are well-known to exhibit chaotic behavior [15], limit cycles (in the absence of damping), and bifurcations [16]. They have been studied by mathematicians, engineers, and physicists for decades, and are often used in the classroom as demonstrations of a practical nonlinear system [17]. They have a variety of practical applications in the controls literature, for example as frameworks representing crane payloads [18]. They also sometimes surface as models of limbs in biomechanics, as in the work of Youn [19]. Even now, their behavior under various types of excitation is the subject of lively academic discourse. For example, the work of Marszal et al. in [20] characterizes bifurcations in the double pendulum when subjected to parameterized vertical excitations of varying amplitude and frequency.

Because the Death Star has the potential to behave like a double pendulum, any misstep on the part of a competitor has the potential to cause the target to move unpredictably. However, the target is not quite as simple as the double pendulum common in controls and dynamics research. Since the plates on the target fall off when hit, the inertial properties of the star change during a typical time trajectory of the target's motion. The analysis of time-varying double pendulum systems is relatively rare in the literature. Some recent work by Gupta [21] sought to characterize double pendulum behavior as a function of mass and length properties, and others such as Bellino et al. [22] have looked at single pendulum systems with time-varying properties, but a system mimicking the star's unique behavior has not been explored. Success in 3-Gun means knocking all of the plates off of the target in the shortest time possible, so the shooter must operate the shotgun in a tight, accurate control loop, minimizing star motion and avoiding critical points in the system's state space.

Competitor strategy is not the focus of this paper, but it is the subject of ongoing inquiry, and the motivation for the present study. The ability to measure the way novice and experienced marksmen and markswomen deal with the unique constraints of this target has the potential to inform a larger body of work on how humans use internal models and develop optimal strategies for path planning and control while balancing risk and reward in unpredictable environments.

The development of an accurate indoor real-time simulation of the target for use in such human motor control experiments is the primary goal of the work in the following pages. Optoelectronic shooting simulators, including devices that simulate "shots" by infrared or light pulses, are not new [23] and are sometimes seen in studies of shooting performance [24, 25]. Some of these studies, such as the work of Swanton in [24], use 3D tracking systems and accelerometers along with optoelectronic target simulators to study shooters' performance. However, no optoelectronic simulator available has the capability to simulate the Death Star, which necessitates the development of a specialized simulator for this target. The simulator hardware and software developed in this study are planned for an open-source release, and are comprised of low-cost, commercially available components, allowing competitors or hobbyists to build their own copy for practice at home, and providing researchers with a platform for future experiments.

To that end, the following sections outline the design of a portable simulator for the Death Star target that accurately represents its dynamic behavior, with virtual plates that fall off when hit with a laser training firearm. First, Section 2 derives the nonlinear, time-varying equations of motion for the target. Then, Section 3 discusses the post-processing of video provided by the 3Gun Nation® television show to calibrate and validate these equations. Finally, Section 4 presents an overview of the implementation of these equations, along with a machine vision algorithm that tracks laser hits on a projected target. Section 5 explores the merits of using the simulator as a training tool for competitive shooters and as a human motor control and perception research platform, including a brief discussion of the range of behaviors that can be expected from the target.

2 Equations of motion

This section will develop a nonlinear state space model for the target to be implemented in section 3. As discussed in Section 1, the star's construction causes it to exhibit behavior similar to a double pendulum whenever less than five and more than zero of the steel plates on the star's arms are attached. However, if the target is allowed to swing in a balanced state with either five or zero plates, only the damping in the star hinge causes angular motion of the star, and the system acts like a standard pendulum. The goal of engaging the target in competitive shooting, of course, is to knock *all* of the plates off of the star. As a result, the target will swing

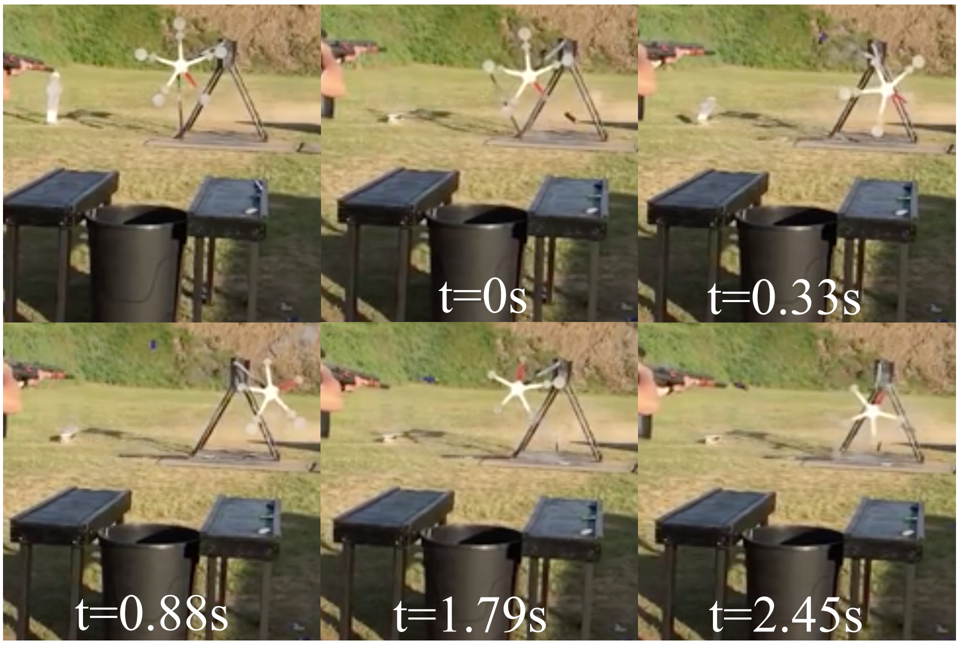

Fig. 1 The Death Star target in motion (video source: 3Gun Nation)

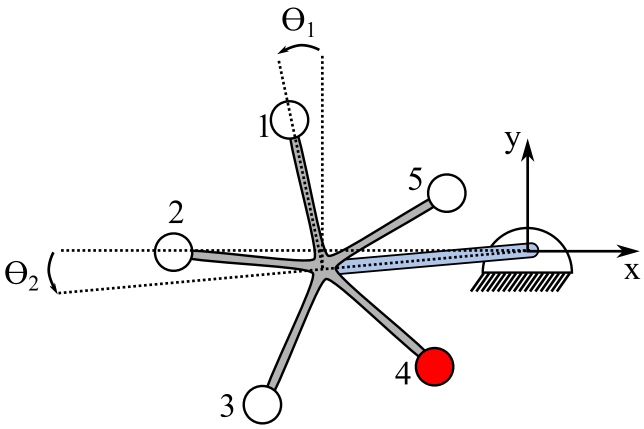

Fig. 2 Coordinates and nomenclature for target

with a varying number of attached plates in varying regions of the state space. For the derivation that follows, the coordinates and nomenclature used can be found in Figure 2.

In Figure 2, θ_1 represents the angle of the star from vertical. θ_2 represents the angle of the swinging arm from a left-pointing horizontal reference. The hinge arm's mass and rotational inertia are small compared to those of the star and plates, and are ignored. The star's rotational inertia and mass are significant, and each plate (numbered 1 through 4) is treated as a point mass in the derivation.

It is worth noting that in competition, the target's swinging motion is initially activated by hitting a secondary steel target which is not shown in Figure 2, but can be seen in the upper leftmost screenshot in Figure 1. This target must be hit before any of the star plates. Additionally, it is stipulated in the 3Gun Nation® competition rules that the bottom rightmost plate of the star must be engaged first. This plate is shown as a colored circle in Figure 2. For the professional shooters using this target in competition, the colored plate is almost always hit before the star begins to move. In fact, this was the case in all validation experiments in Section 3, so each of those simulations simply begins with the removal of this plate at time $t = 0$. However, the real-time simulator discussed in Section 4 does include the activator target for realism.

The equations of motion will be derived using Lagrange's method [26]. The generalized coordinates used are the two angles θ_1, θ_2. Cartesian coordinates x, y are defined as shown in Figure 2, but are only used for developing potential and kinetic energy expressions, and do not appear in the final form of the equations.

An expression for the total kinetic and potential energy of the target system is central to the derivation of the system's equations of motion using Lagrangian dynamics. The Lagrangian of a dynamic system is defined as the difference between the systems kinetic and potential energies, as

$$L = T - V. \tag{1}$$

In Equation 1, T is the system's total kinetic energy, and V is the system's potential energy. As a system moves, the total energy in the system will decrease predictably in the presence of non-conservative generalized "forces" that do work W on the system. The equations of motion for a system can be found by taking the derivative of the Lagrangian according to

$$\frac{d}{dt}\left(\frac{\partial L}{\partial \dot{\theta_k}}\right) - \frac{\partial L}{\partial \theta_k} = \tau_k, \tag{2}$$

where τ_k represents non-conservative torque as mentioned above. For the Death Star target, which is a rotational system with generalized coordinates θ_1 and θ_2, the τ_k in each generalized coordinate comes from friction at the target's two hinges. The non-conservative damping forces from the hinge joints are assumed hereafter to act only as viscous dampers resisting motion, described by

$$\begin{aligned} \tau_1 &= -b_1\dot{\theta}_1 \\ \tau_2 &= -b_2\dot{\theta}_2 - b_1\dot{\theta}_2. \end{aligned} \tag{3}$$

To compute the Lagrangian L, both kinetic and potential energy functions for the moving target must be computed. To make this computation more tractable, consider the following expressions for the position of each portion of the target system in the xy plane,

$$\begin{aligned} x_{st} &= -L_2\cos(\theta_2) \\ y_{st} &= -L_2\sin(\theta_2) \\ x_i &= x_{st} - L_1\sin(\theta_1 + (i-1)\,\alpha) \\ y_i &= y_{st} + L_1\cos(\theta_1 + (i-1)\,\alpha), \end{aligned} \tag{4}$$

where $[x_{st}, y_{st}]$ is the position of the star center, $[x_i, y_i]$ represents the position the plate centers for plate index $i = \{1, 2, 3, 4, 5\}$, and α represents the angular separation of arms, which is always $\frac{2\pi}{5}$ radians for the 5-sided Death Star. Lengths of the star's arms and the swinging arm are L_1 and L_2, respectively. Given expressions for the positions of the plate masses, the potential energy for the system can be computed as

$$\begin{aligned} V &= V_{st} + \sum_{i=1}^{5} V_i \\ V_{st} &= -m_{st}gL_2\sin(\theta_2) \\ V_i &= m_i g\left(-L_2\sin(\theta_2) + L_1\cos(\theta_1 + (i-1)\,\alpha)\right). \end{aligned} \tag{5}$$

This expression for potential energy assumes that the zero reference is for the hinge in the vertical position, with $\theta_2 = \frac{\pi}{2}$. Calculating the system's Lagrangian L as given in Equation 1 also requires an expression for kinetic energy, which is given in mixed rotational and Cartesian coordinates as

$$\begin{aligned} T &= \frac{1}{2}J_{st}\dot{\theta_1}^2 + \frac{1}{2}m_{st}v_{st}^2 + \sum_{i=1}^{5}\frac{1}{2}m_i v_i^2 \\ &= \frac{1}{2}J_{st}\dot{\theta_1}^2 + \frac{1}{2}m_{st}\left(\dot{x}_{st}^2 + \dot{y}_{st}^2\right) + \sum_{i=1}^{5}\frac{1}{2}m_i\left(\dot{x}_i^2 + \dot{y}_i^2\right). \end{aligned} \tag{6}$$

Differentiating the positions of the plate masses in Equation 4 and expressing them in terms of the generalized coordinates θ_1 and θ_2 yields

$$\begin{aligned} \dot{x}_{st} &= L_2\dot{\theta}_2\sin(\theta_2) \\ \dot{y}_{st} &= -L_2\dot{\theta}_2\cos(\theta_2) \\ \dot{x}_i &= L_2\dot{\theta}_2\sin(\theta_2) - L_1\dot{\theta}_1\cos(\theta_1 + (i-1)\,\alpha) \\ \dot{y}_i &= -L_2\dot{\theta}_2\cos(\theta_2) - L_1\dot{\theta}_1\sin(\theta_1 + (i-1)\,\alpha). \end{aligned} \tag{7}$$

With the expressions for the plate velocities now written in terms of the generalized coordinates and their derivatives, the kinetic energy expression of Equation 6 can be rewritten as

$$\begin{aligned} T = \frac{1}{2}\Bigg[&\dot{\theta_1}^2\left(J_{st} + L_1^2\sum_{i=1}^{5}m_i\right) \\ &+ L_2^2\dot{\theta}_2^2\left(m_{st} + \sum_{i=1}^{5}m_i\right) \\ &+ 2L_1L_2\dot{\theta}_1\dot{\theta}_2\sum_{i=1}^{5}\left(m_i\sin(\theta_1 + (i-1)\,\alpha - \theta_2)\right)\Bigg]. \end{aligned} \tag{8}$$

With the kinetic and potential energy totals for the system defined, applying Lagrange's method as defined in Equations 1 and 2 requires taking derivatives of the kinetic and potential energy expressions. To keep the equations compact and readable, consider the introduction of several parameters that show up repeatedly in the equations of motion:

$$\begin{aligned} P_0 &= \sum_{i=1}^{5} m_i \\ P_1 &= \sum_{i=1}^{5} m_i\cos(\theta_1 + (i-1)\,\alpha - \theta_2) \\ P_2 &= \sum_{i=1}^{5} m_i\sin(\theta_1 + (i-1)\,\alpha - \theta_2) \\ P_3 &= P_0 + m_{st} \\ P_4 &= \sum_{i=1}^{5} m_i\sin(\theta_1 + (i-1)\,\alpha). \end{aligned} \tag{9}$$

Using these parameters for convenience, performing the derivatives in Equation 2 for θ_1 and substituting the non-conservative forces in Equation 3 leads to

$$\begin{aligned} -b_1\theta_1 &= \ddot{\theta}_1\left(J_{st}+L_1^2P_0\right)+L_1L_2\ddot{\theta}_2P_1 \\ &\quad - L_1L_2\dot{\theta}_2\left(\dot{\theta}_1-\dot{\theta}_2\right)P_2-\frac{\partial L}{\partial \theta_1}. \end{aligned} \tag{10}$$

For readability, $\frac{\partial L}{\partial \theta_1}$ will not be expanded in the final equations, but is given by

$$\frac{\partial L}{\partial \theta_1} = L_1L_2\dot{\theta}_1\dot{\theta}_2P_1 + L_1gP_4. \tag{11}$$

The same procedure can be repeated for θ_2, and reduces to

$$\begin{aligned} -b_2\dot{\theta}_2 - b_1\dot{\theta}_2 &= L_2^2\ddot{\theta}_1P_3 + L_1L_2\ddot{\theta}_1P_2 \\ &\quad + L_1L_2\dot{\theta}_1\left(\dot{\theta}_1-\dot{\theta}_2\right)P_1 - \frac{\partial L}{\partial \theta_2}. \end{aligned} \tag{12}$$

As in Equation 10, $\frac{\partial L}{\partial \theta_2}$ is not expanded explicitly in Equation 12 but is given by

$$\frac{\partial L}{\partial \theta_2} = L_1L_2\dot{\theta}_1\dot{\theta}_2P_2 + L_2g\cos\theta_2P_3. \tag{13}$$

When rearranged, these equations become recognizable as the equations of motion for the target system:

$$\begin{aligned} \ddot{\theta}_1 &= \frac{1}{\left(J_{st}+P_0L_1^2\right)\left(1-\frac{P_1^2}{P_0P_3}\right)}\times \\ &\left[\frac{\partial L}{\partial \theta_1} - \left(b_1+b_2\right)\dot{\theta}_1 + L_1L_2\left(P_2\dot{\theta}_2\left(\dot{\theta}_1-\dot{\theta}_2\right)\right.\right. \\ &\left.\left. -\frac{P_1}{L_2^2P_3}\left(P_2L_1L_2\dot{\theta}_1\left(\dot{\theta}_1-\dot{\theta}_2\right)+\frac{\partial L}{\partial \theta_2}-b_2\dot{\theta}_2\right)\right)\right] \\ \ddot{\theta}_2 &= \frac{1}{P_3L_2^2\left(1-\frac{P_1^2}{P_0P_3}\right)}\times \\ &\left[\frac{\partial L}{\partial \theta_2} - b_2\dot{\theta}_2 + L_1L_2\left(P_2\dot{\theta}_1\left(\dot{\theta}_1-\dot{\theta}_2\right)\right.\right. \\ &-\frac{P_1}{L_1^2P_0}\left(P_2L_1L_2\dot{\theta}_2\left(\dot{\theta}_1-\dot{\theta}_2\right)+\frac{\partial L}{\partial \theta_1}\right. \\ &\left.\left.\left. -\left(b_1+b_2\right)\dot{\theta}_1\right)\right)\right]. \end{aligned} \tag{14}$$

With these equations for the acceleration of the star in the generalized coordinates θ_1 and θ_2, a nonlinear state space model of the system is easily constructed so that the equations may be solved using a numerical integration technique. The state space model is constructed using the state vector

$$\mathbf{x} = \left[\theta_1\ \dot{\theta}_1\ \theta_2\ \dot{\theta}_2\right]^T. \tag{15}$$

This state vector is used to rearrange the expressions for $\ddot{\theta}_1$ and $\ddot{\theta}_2$ in Equation 14 into the state space form,

$$\frac{d\mathbf{x}}{dt} = \mathbf{f}(\mathbf{x}, t). \tag{16}$$

The implementations of Equation 16 in this study were solved using a second order Runge Kutte (Heun's) method. In Heun's method, sometimes called the explicit trapezoidal rule [27], an intermediate guess for the value of the state vector is calculated using an Euler approximation, and then corrected in a secondary step. This method can be summarized as

$$\begin{aligned} \tilde{\mathbf{x}}(k+1) &= x_i(k) + Tf(\mathbf{x}(k), t(k)) \\ \mathbf{x}(k+1) &= x(k) + \frac{T}{2}\left[f(\mathbf{x}(k), t(k))\right. \\ &\qquad \left. + f(\tilde{\mathbf{x}}(k+1), t(k+1))\right], \end{aligned} \tag{17}$$

where T is the simulation timestep, $f(\mathbf{x}(\mathbf{k}), t(k))$ are the time-varying equations for the state derivatives in Equation 16, and $\tilde{\mathbf{x}}(\mathbf{k+1})$ is the "intermediate" value of the state vector. This method was chosen because it is easy to implement in real-time, and allows for easy updates of the system properties as plates on the star are hit and fall off.

In simulation of the equations of motion derived in this section, "hitting a plate" at a particular time step k results in the simulation setting that plate's mass to 0 for the next simulation update. The practice of simply setting a plate's mass to 0 implicitly updates the system's kinetic and potential energy by changing the target's moment of inertia and mass center location. Because the projectiles from a competitor's shotgun impart momentum to the departing plate orthogonal to the generalized coordinates θ_1 and θ_2, the impulse on the target from the shot cloud can be ignored. The assumption that the plates fall off instantaneously is certainly a substantial simplification, and is discussed further in Section 3.

3 Experimental Validation

In order to develop a simulation environment for studying the interaction between competitor and target, Equation 14 must be calibrated and validated against the actual target's motion. In lieu of constructing a modified, instrumented version of the target for validation, video from the 3Gun Nation® television show featuring the target was obtained from its producers. By analyzing the video, the target motion was extracted for comparison to the system equations. This method allows for validation of the equations in as realistic a setting as possible. The target's potential to act erratically is

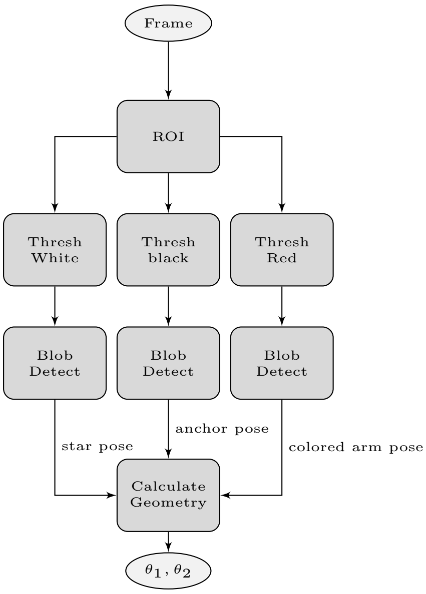

Fig. 3 Image processing pipeline for extracting target motion from video

smoke, or airborne spent shotgun hulls in the frame. These were corrected by manually clicking on the reference points in the image when necessary, rather than relying on interpolation or median filtering. Generally, however, the tracking methodology was reliable for the video data processed below.

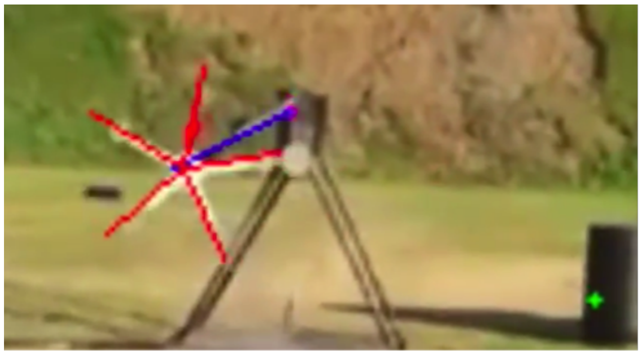

Fig. 4 Python/OpenCV star tracking program output image

its hallmark, and confirming that the equations capture the interesting behavior of the real target would be ideal. However, it is far more manageable to validate the system equations in the portions of the state space that are most common during competition. Thus, using actual competition footage to validate the equations has significant advantages.

A post-processing pipeline was developed in Python and OpenCV [28] to track the target's motion. The background at a firing range is relatively predictable in color and texture, and the target is painted in high-contrast colors. Therefore, after loading each frame and cropping it to a suitable Region of Interest (ROI), color segmentation, thresholding, and blob detection in OpenCV provided locations for the star centroid, the centroid of the colored "activator" arm of the star, and the centroid of a fixed object on the range. Camera motion was subtracted from target motion using the fixed "anchor" object, and the centroids of the star and the colored arm provided measurements of θ_1 and θ_2 respectively. Figure 3 shows a block diagram of the image processing pipeline.

Admittedly, this pipeline is only designed to work with videos sourced from the 3Gun Nation® television show. While this may seem limiting, the show's footage covers most of the target's use in competition as of 2015. In the shooting matches featured on the television show, the target is always painted the same way, and the lighting conditions are always similar. Figure 4 shows a sample of the output from the Python image processing program. Occasional outlier points in the tracking results occured due to occlusions from dust,

In addition to the automated process of tracking star motion, it is also necessary to detect when shots are fired and when plates fall off of the target to give a simulation the information it needs to update the target's inertial properties. To simplify this process, a trial in which five shots resulted in five hits was analyzed. This way, the audio waveform from the video file was processed using Python and a simple volume thresholding algorithm to detect shots at particular points in time during the video. Because of the delay between the shot and when the shot cloud knocks the plate off of the spinning star, a delay between detected shot times and changes in the star's mass properties was implemented in simulation. This delay was experimentally determined to be roughly $0.1s$ by manually scrolling through video frames in collected video data, noting the number of frames between when a shot was heard and when the hit plate left the spinning star.

To use the equations developed in Section 2 in a validation experiment, the target's physical dimensions, damping characteristics, and inertial properties must be matched to those of the actual star. The parameters used in simulation are summarized in Table 1. All of the parameters shown in the table other than the two damping values were estimated using dimensions from drawings and pictures provided by 3Gun Nation® personnel.

The damping values shown in Table 1, b_1 and b_2, were not readily available, so they were estimated. Hinge damping b_2 was estimated by tracking the star's motion during video of a special case of target motion. In this clip, the star's motion was tracked for several swings

Table 1 "Death Star" measured and calculated parameters

Variable	Description	Value	Units
L_1	star arm length	0.73	m
L_2	hinge arm length	0.80	m
b_1	star bearing damping	1.03	$Nm \cdot s$
b_2	hinge bearing damping	1.03	$Nm \cdot s$
m_{st}	star mass	24.45	kg
m_i	plate mass	2.50	kg
J_{st}	star rotational inertia	1.26	$kg \cdot m^2$

after all of the targets had been hit. In this type of scenario, the target swings in a balanced state. If this type of motion is modeled as a simple single pendulum of length L_2 and the star's inertia is modeled as a point mass, the system can be approximated by a second order differential equation, and can be linearized about the vertical resting condition at $\theta_2 = 90°$. The linearized equation of motion for such a pendulum is

$$\ddot{\theta}_2 = -\frac{b_2}{m_{st}L_2^2}\dot{\theta}_2 - \frac{g}{L_2}\theta_2, \tag{18}$$

and has characteristic equation

$$s^2 + \frac{b_2}{m_{st}L_2^2} + \frac{g}{L_2} = 0 = s^2 + 2\zeta\omega_n + \omega_n^2. \tag{19}$$

The rightmost side of Equation 19 shows the standard form for second order underdamped systems with natural frequency ω_n and damping ratio ζ. Using the logarithmic decrement formula

$$\zeta = \frac{\frac{1}{n-1}ln(\frac{y_1}{y_n})}{\sqrt{4\pi^2 + (\frac{1}{n-1}ln(\frac{y_1}{y_n}))^2}}, \tag{20}$$

as found in many system dynamics texts, including [29], the approximate damping ratio ζ for this system can be found by examining the amplitude of the hinge angle at subsequent peaks. The damping ratio of the approximate second-order pendulum representation of the hinge motion was found to be $\zeta = 0.0083$, and the approximate natural frequency ω_n was found to be $3.43\frac{rad}{s}$. These values were used along with Equation 19 to yield the rough estimate for b_2 shown in Table 1.

The only remaining unknown parameter, b_1, or the damping of the star hinge, was assumed to be the same as the damping in the swinging arm hinge, since similar bearings were used for each in the construction of the physical target.

To assess how the model and the data compare, a high-speed $240fps$ video of a competitor's run on the target was obtained from 3Gun Nation ® staff. In this clip, the target engagement order was 4,1,5,2,3, and the star began to move just after target 4 was engaged. The match between model and data for this run is shown in Figure 5. The cosample deviation between the model's predictions and the video data for the trial shown in Figure 5 is $0.109rad(6.25°)$ for θ_2 and $0.274rad(15.70°)$ for θ_1. Given the coarse data collection method and the fact that the model neglects coulomb friction and hinge arm inertial properties, these numbers are fairly good.

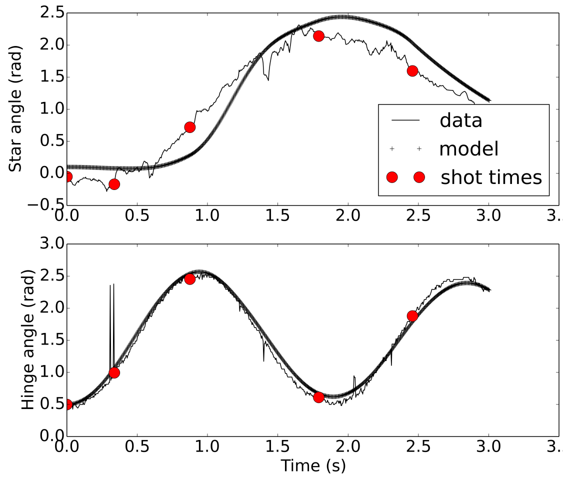

Fig. 5 Model vs. measured target motion for one recorded trial. Plates engaged in order 4,1,5,2,3

As Figure 5 shows, the predicted hinge angle θ_2 matches the experimental data better than star angle θ_1. This agrees with intuition; the star is massive compared to the plates, so this portion of the system can be expected to act similarly to a standard pendulum. This is especially true since this trial represents particularly fast shooting, meaning that the unbalanced star has little time to influence the system dynamics. Shot times are indicated in Figure 5 by circles overlaid on the measured angles. The star angle is a far less precise match. This has several possible causes. Plates are assumed in simulation to fall off of the star instantaneously after being hit by a cloud of shotgun pellets, and individual plate masses in the simulation are set to zero at the timestep of the identified hit. In reality, the plates' departure takes time, and may influence star dynamics. The assumption of ideal, linear viscous damping is also a potential source of error, considering that most bearings are subject to varying degrees of nonlinear coulomb friction. Finally, the video processing algorithm itself is subject to errors due to slight lighting and color changes during the video.

In Figure 5, the competitor was able to hit all of the star's targets quickly, and used a very strategic order of target engagement, always hitting the plate with the largest potential energy (highest from the ground).

This is a strategy that was quickly adopted by top competitors during the 2015 season of the 3Gun Nation ® professional shooting series, but not all competitors shot the target the same way. In the first pro series event of the 2015 season, one competitor engaged the targets in the order 4,5,3,2,1. Using footage from the television show, obtained in the form of high definition $23fps$ video, the match between model and data for this run was obtained. The match is shown in Figure 6.

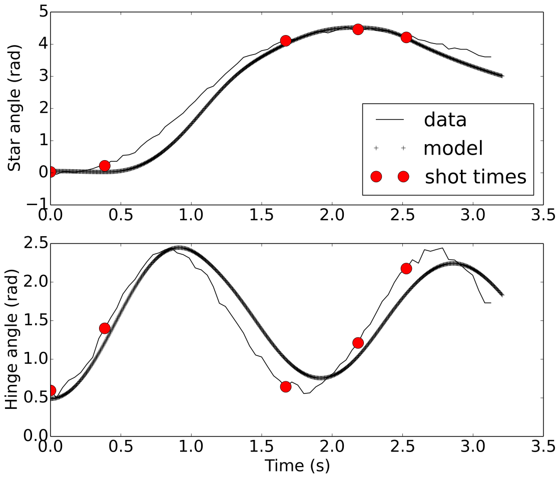

Fig. 6 Model vs. measured target motion for one recorded trial. Plates engaged in order 4,5,3,2,1

Figure 6 also shows good agreement between model and data, with a cosample deviation of $0.240rad$ for hinge angle and $0.238rad$ for star angle. The raw numbers show that there is more error in this trial than in the trial represented by Figure 5, but the gross behavior of the target is still captured well. In general, the simulation replicates the magnitude and shape of the target's response for relatively short trials where competitors are successful in hitting a plate with every shot. Because of the target's similarity to a double pendulum, however, bifurcations in behavior are possible, and the system is very sensitive to initial conditions and thus shot times in certain regions of the state space.

To show the limitations of the simulation's fidelity, a third comparison of data and simulation was performed. Like the other two trials shown in Figures 5 and 6, the hinge began to swing just after plate 4 was hit. In this trial, however, the competitor missed several plates, resulting in a particularly slow time. This gave the target's dynamics time to evolve in an unbalanced state, increasing the influence of shot time on the target's motion. Additionally, the hits on several of the plates were not "clean," meaning that an off-center hit caused the plate to take a relatively long time to leave the star arm. Recall that the initial condition sensitivity of the target's equations of motion means that small changes in the timing of each individual shot (or rather, the timing of the plates leaving the star) can have drastic effects on the eventual evolution of the target's states θ_1 and θ_2, since individual mass positions and velocities have errors that compound with small errors in each shot time. The results of the third validation experiment are shown in Figure 7. To show the effects of relatively small changes in shot time on the match between model and data, a second simulation was compared to the same data in which the third plate's departure from the star was artificially delayed from the measured time by a mere 4 frames of $23fps$ television show footage. Compounded by the modeling assumptions, particularly those of zero coulomb friction and instant plate departure, initial condition and shot time variability has a large effect on the match between data and simulation.

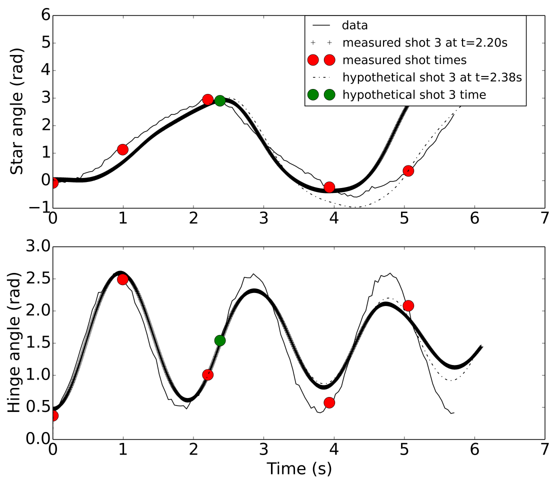

Fig. 7 Model vs. measured target motion for one recorded trial. Plates engaged in order 4,1,5,3,2

The poor agreement in Figure 7 using the measured plate 3 departure time may lead readers to wonder whether the parameters in Table 1 and the state space equations in Equation 14 can be used to predict target motion reliably for any set of shot times in a trial any target engagement order. This type of universal agreement would be ideal, but is hardly realistic given the sources of variability in the human-shotgun-target closed-loop system and the modeling assumptions mentioned above. In fact, Figure 7 shows that the initial condition sensitivity of the equations alone, which is explored further in Section 5, can result in vastly dif-

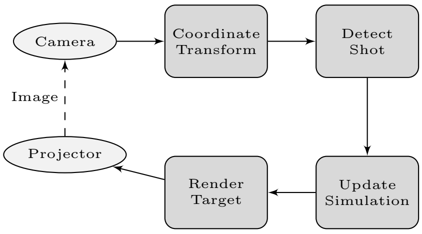

Fig. 8 Laser-activated simulator program loop structure

ferent target behavior for small changes in shot time. Fortunately, the results in the above experiments still provide support for the hypothesis that the state space system in Equation 14 is effective for predicting the gross behavior of the target for a range of target engagements. Therefore, this model is employed in Section 4 to develop a real-time optoelectronic simulator for use in competitor training.

4 Simulator Design

After building the calibrated state space model presented in Section 3, the equations of motion for the target were used in the construction of an indoor, real-time simulation of the target that allows competitors to shoot the star with an inert laser training firearm. The simulator system is driven by a program written in the Python programming language using both the OpenCV [28] and PyGame libraries that simulates the target's motion and tracks laser hits on a projected image of the simulation using a multi-threaded program structure. Physically, the simulator consists of a Microsoft® webcam modified with a near infrared-pass filter and permanently affixed to a Gigabyte® "mini-box" style PC with a built-in projector running Ubuntu® Linux. The thread in the Python program simulating target motion at 60Hz calculates the target's states at each timestep using the state space model in Equation 14. The camera provides images to the image processing thread at roughly 30 frames per second. When available, each camera image is scaled and cropped so that image coordinates align with projector coordinates. Then, a brightness thresholding algorithm is performed on the captured near infrared image to detect laser hits. A latch, or rising edge detection algorithm, is employed so that successive frames do not result in successive detected hits. Hit locations are compared with time-delayed plate locations according to the target motion simulation to compensate for image acquisition delay (roughly 0.1 seconds), and plate masses are removed from the system equations as they are hit. Figure 8 shows an outline of the simulator software/hardware pipeline.

Each of the rectangular blocks in Figure 8 represents a subroutine in the Python program's image processing thread. The faster, $60Hz$ simulation thread uses the latest data from the image processing thread to update the target's dynamics and render them smoothly for the simulator's user. Image acquisition is performed using OpenCV's built-in camera capture functionality. The target's motion is activated when the user hits the colored plate, which takes the place of the activator target in the real system. Elapsed time for each shot is displayed in the upper left corner of the projected image along with a target that resets the program, but otherwise the rendering of the target is minimal to prevent visual distraction for a user. Figure 9 shows the physical system, which boots and starts a full-screen simulation when turned on.

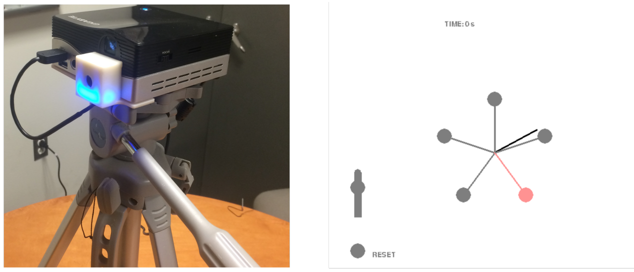

Fig. 9 Laser activated simulator and projected image (brightness inverted)

This simulator has been tested for reliability in indoor, even lighting. With the release of hardware and software designs to the open source community, the author expects the system to continue to be refined, and provide valuable practice to competitors as well as a platform for future research efforts to study the dynamics of the complex closed-loop target-shooter sytem. In a research setting, its open source software can be easily combined with other sensors such as eye tracking systems, motion tracking camera systems, and/or inertial sensors to provide a fully instrumented experimental environment similar to what was developed by Swanton in [24].

5 Discussion and Conclusions

This paper described the modeling, simulation, and validation of the 3-Gun Nation Death Star shotgun target, and outlined the development of a real-time optoelectronic simulation environment. The simulator will be released as an open source project to facilitate competitor practice, and will be used as a research platform in experiments directed at analyzing competitor strategy, planning, and movement while interacting with the target in competition. The equations of motion developed in Section 2 were validated against video data from an actual 3-Gun competition, indicating their usefulness in replicating target motion in the laser-activated simulator. It is the hope of the author that this simulation framework will lead to experiments that investigate the way human motor control systems deal with complex, nonlinear targets in goal-directed aiming. To facilitate this type of formal experiment, the simulator stores all relevant data while trials are being completed to a text file that is easy to load into common software packages for post-processing. Data from a sample trial using the optoelectronic simulator is shown in Figure 10.

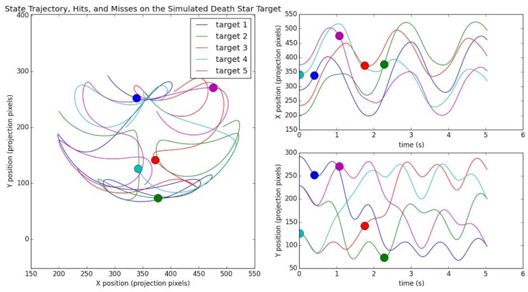

Fig. 10 Sample data provided by the optoelectronic simulator during a trial.

The data in Figure 10 include information about the timing and location of each laser hit, along with the time-trajectory of each plate during the trial. In combination with a synchronized eye tracking system, the data provided by the simulator could be just as useful in theoretical studies of human motor control as in a practice session for a 3-Gun competition. All of the inertial, spatial, and damping characteristics of the target, as well as the position and delay offered by the activator target, are adjustable.

In Section 3, the third validation experiment showed evidence of the target's sensitivity to the timing of hits on each plate. Because this is one of the key characteristics of this target's challenge for competitors, it is worth pointing out just how sensitive the equations really are. To further examine the target's potential for unpredictable behavior within the scope of human error, consider Figure 11. In this hypothetical scenario, simulated offline using Equation 14, a simulated competitor chose to engage targets 4,3, and 2. Target 2's departure, marked by the third shot, was delayed by 0.01 seconds for five separate runs of the simulation. It is clear that even this small difference in timing has large effects on the subsequent motion of the target. Figure 11 shows the target in an initial condition-sensitive region of the state space, and also highlights a bifurcation in the system dynamics. For the last two trials, the star spun all the way around rather than swinging downwards as it did for the first three trials. This phenomenon makes learning to shoot the Death Star effectively extremely hard, and also illustrates the difficulty of ensuring a match between simulations and target motion measured using video of competitition, as in Section 3. Obviously, in the case of Figure 11, a better strategy in choosing target order could have helped avoid this type of behavior, but learning the best way to shoot the target takes practice. Presumably, a competitor uncovering this apparent unpredictability would learn to engage targets in an order that minimizes the chance of exciting a bifurcation or otherwise difficult-to-predict state trajectory. The implications of these choices, variability in shooter performance, and optimal strategies are subjects of ongoing study.

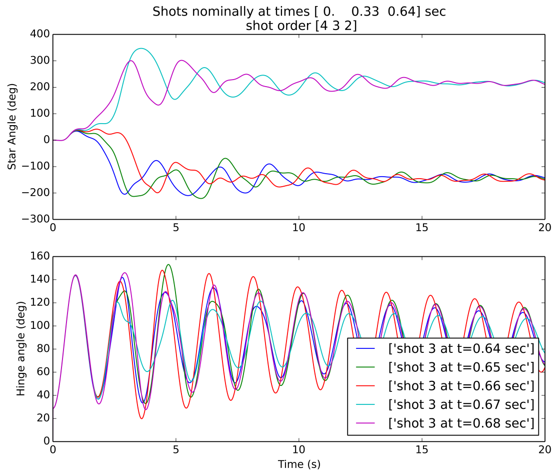

Fig. 11 Simulation in which three targets were engaged in the order 4,3,2, for various timing of the third shot.

References

1. Causer, J., Bennett, S.J., Holmes, P.S., Janelle, C.M., Williams, A.M.: Quiet eye duration and gun motion in elite shotgun shooting. Medicine & Science in Sports & Exercise **42**(8), 1599–1608 (2010)
2. Causer, J., Holmes, P.S., Smith, N.C., Williams, A.M.: Anxiety, movement kinematics, and visual attention in elite-level performers. Emotion **11**(3), 595 (2011)
3. Rauterberg, M.: Emotional effects of shooting activities:'real'versus' virtual'actions and targets. In: Proceedings of the second international conference on Entertainment computing, pp. 1–8. Carnegie Mellon University (2003)
4. Dadswell, C., Payton, C., Holmes, P., Burden, A.: The effect of time constraints and running phases on combined event pistol shooting performance. Journal of Sports Sciences (ahead-of-print), 1–7 (2015)

5. Vickers, J.N., Williams, A.M.: Performing under pressure: The effects of physiological arousal, cognitive anxiety, and gaze control in biathlon. Journal of Motor Behavior **39**(5), 381–394 (2007)
6. Baca, A., Kornfeind, P.: Stability analysis of motion patterns in biathlon shooting. Human movement science **31**(2), 295–302 (2012)
7. Gillingham, R., Keefe, A.A., Keillor, J., Tikuisis, P.: Effect of caffeine on target detection and rifle marksmanship. Ergonomics **46**(15), 1513–1530 (2003)
8. Share, B., Sanders, N., Kemp, J.: Caffeine and performance in clay target shooting. Journal of sports sciences **27**(6), 661–666 (2009)
9. Ball, K., Best, R., Wrigley, T.: Body sway, aim point fluctuation and performance in rifle shooters: inter-and intra-individual analysis. Journal of sports sciences **21**(7), 559–566 (2003)
10. Tremayne, P., Barry, R.J.: Elite pistol shooters: physiological patterning of best vs. worst shots. International journal of psychophysiology **41**(1), 19–29 (2001)
11. Ball, K.A., Best, R.J., Wrigley, T.V.: Inter-and intra-individual analysis in elite sport: Pistol shooting. Journal of Applied Biomechanics **19**(1), 28–38 (2003)
12. Hoffmann, E.R.: Capture of moving targets: a modification of fitts' law. Ergonomics **34**(2), 211–220 (1991)
13. Tresilian, J.R.: Hitting a moving target: perception and action in the timing of rapid interceptions. Perception & Psychophysics **67**(1), 129–149 (2005)
14. Slotine, J.J.E., Li, W., et al.: Applied nonlinear control, vol. 199. Prentice-hall Englewood Cliffs, NJ (1991)
15. Shinbrot, T., Grebogi, C., Wisdom, J., Yorke, J.A.: Chaos in a double pendulum. Am. J. Phys **60**(6), 491–499 (1992)
16. Yu, P., Bi, Q.: Analysis of non-linear dynamics and bifurcations of a double pendulum. Journal of Sound and Vibration **217**(4), 691–736 (1998)
17. Calvão, A., Penna, T.: The double pendulum: a numerical study. European Journal of Physics **36**(4), 045,018 (2015)
18. Vaughan, J., Kim, D., Singhose, W.: Control of tower cranes with double-pendulum payload dynamics. Control Systems Technology, IEEE Transactions on **18**(6), 1345–1358 (2010)
19. Youn, S.H.: Double pendulum model for tennis stroke including a collision process. arXiv preprint arXiv:1505.01916 (2015)
20. Marszal, M., Jankowski, K., Perlikowski, P., Kapitaniak, T.: Bifurcations of oscillatory and rotational solutions of double pendulum with parametric vertical excitation. Mathematical Problems in Engineering **2014** (2014)
21. Gupta, M.K., Bansal, K., Singh, A.K.: Mass and length dependent chaotic behavior of a double pendulum. In: Advances in Control and Optimization of Dynamical Systems, vol. 3, pp. 297–301 (2014)
22. Bellino, A., Fasana, A., Gandino, E., Garibaldi, L., Marchesiello, S.: A time-varying inertia pendulum: analytical modelling and experimental identification. Mechanical Systems and Signal Processing **47**(1), 120–138 (2014)
23. Mononen, K., Viitasalo, J., Era, P., Konttinen, N.: Optoelectronic measures in the analysis of running target shooting. Scandinavian journal of medicine & science in sports **13**(3), 200–207 (2003)
24. Swanton, A.: Development of a recording system to empirically analyse the shooting characteristics of olympic trap clay target shooters. Master's thesis, University of Limerick (2011)
25. Zanevskyy, I., Korostylova, Y., Mykhaylov, V.: Specificity of shooting training with the optoelectronic target. Acta of Bioengineering and Biomechanics **11**(4), 63–70 (2009)
26. Moon, F.C.: Applied dynamics: with applications to multibody and mechatronic systems. John Wiley & Sons (2008)
27. Ascher, U.M., Petzold, L.R.: Computer methods for ordinary differential equations and differential-algebraic equations, vol. 61. Siam (1998)
28. Itseez: Open source computer vision library. https://github.com/itseez/opencv (2015)
29. Kulakowski, B.T., Gardner, J.F., Shearer, J.L.: Dynamic modeling and control of engineering systems. Cambridge University Press (2007)